Journal of Hydrology (NZ) 54 (1): 33-52 2015

Seasonal infiltration and groundwater movement in schist bedrock, Southern Alps, New Zealand

Alex Sims,[1] Simon C. Cox,[2] Sean Fitzsimons[1] and Peter Holland[1]

[1] *Department of Geography, University of Otago, PO Box 56, Dunedin, New Zealand. Corresponding author: alexsims87@gmail.com*

[2] *GNS Science, Private Bag 1930, Dunedin 9054, New Zealand*

Abstract

The amount of precipitation that infiltrates mountain bedrock is poorly quantified, yet known to strongly influence alpine stream baseflow, landslide initiation, lowland aquifer recharge and, potentially, fault strength. Groundwater discharge in a 355 m tunnel through the western flank of the Southern Alps, New Zealand, was monitored from April 2012 to January 2013 and compared with rainfall records at a nearby rain gauge in order to advance understanding of rainwater infiltration into schist bedrock. Tunnel discharge responded rapidly to 21 distinct rainfall events, with their discharge hydrographs characterised by steeply rising limbs and exponential declines following peak discharges. Two anomalous discharge events (ADE) were recorded when discharge increased despite the absence of associated rainfall. A significant ADE during July 2012 is attributed to snowmelt. Calculated cumulative tunnel discharge and proportions of rainfall infiltration (derived from rainfall versus discharge) indicate that from September 2012 to January 2013 greater volumes of water entered the tunnel, per unit of rainfall, than from April to August 2012. Differences in the magnitude and timing of peak discharge relative to rainfall were also observed between the two periods. Differences in volume and flow rate are thought to reflect seasonal rise of the water table intersecting the tunnel to induce lateral flow and elevate observed discharge. Estimates of the proportion of rainfall that infiltrated bedrock vary between events, from 0.3 to 20%.

Keywords

infiltration, Southern Alps, groundwater, Alpine Fault, snowmelt, rainfall, Tatare Tunnel

Introduction

Precipitation that falls on mountains can give rise to runoff, evaporation, infiltration and short or long term storage of water as snow or ice. Topographic relief provides a strong driving force for infiltration of meteoric water into the rock mass of a mountain belt (Koons and Craw, 1991; Menzies *et al.,* 2014). Once inside, these fluids play an important role in collisional processes through the transport of heat and mass (Bickle and McKenzie, 1987), or by changing the strength of faults and the rheological behaviour of the crust (Wintsch *et al.*, 1995). The impact of infiltration on crustal deformation and mountain building depends on the volume of fluid involved, its source, the flow path, temperature, and the characteristics of fluid-rock interaction at different levels in the crust (Yardley, 2009). Recent studies suggest that the incursion of meteoric water reaches as far as the ductile regime in an active orogen (Menzies *et al.*,

2014). Although the brittle upper crust is likely to be saturated with surface-derived water, the total flux and relative contributions of different fluid sources are, on the whole, poorly quantified.

Controls on infiltration and the responses of groundwater to recharge events are complicated and often paradoxical (Kirchner, 2003). The style of response is dependent on rock mass permeability and its capacity to buffer infiltration through groundwater storage. While the flux rate of infiltrating water is generally low, the timeframe for response may be orders of magnitude faster (Rasmussen *et al.,* 2000). Two fundamental concepts account for variations in groundwater response and infiltration: velocity-type responses (where response time and magnitude are controlled by the velocity of water moving through sub-surface flowpaths) and responses controlled by celerity (where a perturbation is transmitted much more rapidly through a saturated medium, in a similar manner to a flood or pressure wave propagating downstream in a river) (McDonnell and Beven, 2014). Variations in rock mass saturation, storage capacity and antecedent recharge make distinguishing between these controls difficult. These complications do not, however, preclude first-order estimates of the timeframes and patterns of groundwater responses to infiltration. This study seeks to bring a fresh perspective to this issue by documenting the shallow infiltration of meteoric water in the Southern Alps of New Zealand.

The Southern Alps are part of a relatively young mountain belt in the actively deforming hanging wall of the Alpine Fault, where the Pacific plate has been uplifted to an altitude of >3000 m across the path of the prevailing westerly winds blowing from the Tasman Sea and the Southern Ocean. The result is a strongly asymmetric pattern of weather, erosion and crustal deformation reaching towards worldwide extremes (Cox *et al.*, 2012; Cox and Sutherland, 2007). Orographic forcing on the windward (western) side of the Southern Alps results in: rainfall exceeding 10,000 mm/year, with storm rainfall intensity in the order of (up to) 100 mm/hour (NIWA, 2014); runoff with suspended sediment yields exceeding 100 t/m^2/year (Hicks *et al.*, 2011); rapid uplift at rates > 10 mm/year (Cox and Sutherland, 2007); and localised crustal deformation (Koons *et al.*, 1998; Koons *et al.*, 2003). The intense orographic rainfall means that infiltration and runoff budgets are likely to be amplified compared with, for example, evapotranspiration, thereby providing an ideal situation in which to characterise infiltration.

The proportion of precipitation that becomes runoff is by far the best understood component of the Southern Alps' hydrological cycle, primarily because of the abundance of stream gauging sites and the power of rainfall-runoff modelling (Ibbitt *et al.,* 2001). Although other components are understood at the hydrological scale, infiltration is rarely quantified. In the Southern Alps, infiltration of meteoric water and its subsequent shallow circulation are important drivers of baseflow in alpine streams. Fluids also play a role in landslide initiation and in the wider hydrological cycle (De Vita *et al.*, 1998; Glade, 1998).

The rockmass above Tatare Tunnel is a relatively homogeneous fractured schist, with permeability of between 10^{-15} and 10^{-12} m^2 (Cox *et al.*, 2015). On a timescale of months, years, or longer, rates and patterns of infiltration are also expected to control the availability of groundwater and fluid circulation in and around the Alpine Fault, and may even have a bearing on its strength and earthquake rupture behaviour (Sutherland *et al.*, 2012). Furthermore, schist on the western flanks of the Southern Alps (Cox and Barrell, 2007) is being rapidly uplifted and its permeability is expected to

reflect the interaction of topographic and tectonic stresses (Upton and Sutherland, 2014).

The principal aim of this study was to document the nature and proportion of precipitation that infiltrates schist bedrock to become groundwater along the western flanks of the Southern Alps. The research involved measurements in Tatare Tunnel near Franz Josef township. This unlined 355 m tunnel was excavated in the 1890s through schist bedrock typical of the western Southern Alps. Tunnel discharge was measured during the nine months from April 2012 to January 2013. This period included a significant snowfall (27 June 2012) and a 10-year storm event (1-3 January 2013). Tunnel discharge from 21 distinct storm cycles (referred to here as discharge events) was compared with rainfall records from a NIWA rain gauge located 7 km north east of the tunnel at an elevation of 90 m above mean sea level (msl). A simple numerical model was applied to the rainfall and discharge data to allow comparison of infiltration patterns between discharge events. While it was beyond the scope of this study to complete a water budget, the findings are expected to deepen our understanding of shallow groundwater flow and the links between precipitation and groundwater flow in the Southern Alps, New Zealand.

Study site

Tatare Tunnel lies 2 km east of Franz Josef township at an elevation of 265 m above msl. The tunnel is unlined, approximately 1 m wide and 2 m high, and slopes downwards ~ 0.3° towards its western outlet. It was excavated by hand during an operation to bring water to an unsuccessful gold sluicing operation in the late 1890s, and was used after 1938 to generate hydroelectric power for Franz Josef. It is now disused but serves as a popular local tourist attraction. A low mound and a wooden aquaduct prevent water entering the tunnel at its uphill end. Water does, however, enter through cracks and seeps in the schist bedrock, and gathers into a flowing stream on the tunnel floor, then exits via a steel half-pipe set into the tunnel bed at its western outlet. The length and orientation of the tunnel mean that measurements taken at the outflow characterise total groundwater flow through a relatively thick section (355 m) of rock oriented approximately at right angles to the Alpine Fault (Fig. 1). Overburden varies between 5 m and 90 m along the length of the tunnel and is thickest near the eastern portal (Fig. 2). Menzies (2012) determined, using analyses of the stable isotopes ^{18}O and ^{2}H (referred to as D in Appendix B), that water entering the tunnel was meteoric in origin and unexchanged with the surrounding schist bedrock. These findings are supported by the stable isotope analyses conducted for this study (Fig. B1) and rule out alternative fluid sources (for example thermal springs), supporting the contention that precipitation drives discharge in the Tatare Tunnel.

The bedrock is predominantly quartzo-feldspathic schist concordantly interlayered with minor (approximately 1 cm thick) bands of mafic amphibolite, metachert and concordant to discordant veins of quartz. The schist is strongly laminated, with a relatively constant 60-70° southeast-dipping schistosity (mean 137°/63° dip direction/dip) oriented at a steep angle to the tunnel. Flow of groundwater in the rock mass is through fractures, with those at a high angle to foliation tending to have wider apertures and higher flux rates than those nearly parallel to foliation. Based on a compilation of available data, Cox *et al.* (2015) suggested that the >10 m-scale (intrinsic) fracture permeability of the schist is likely to be between 10^{-15} and 10^{-12} m^2.

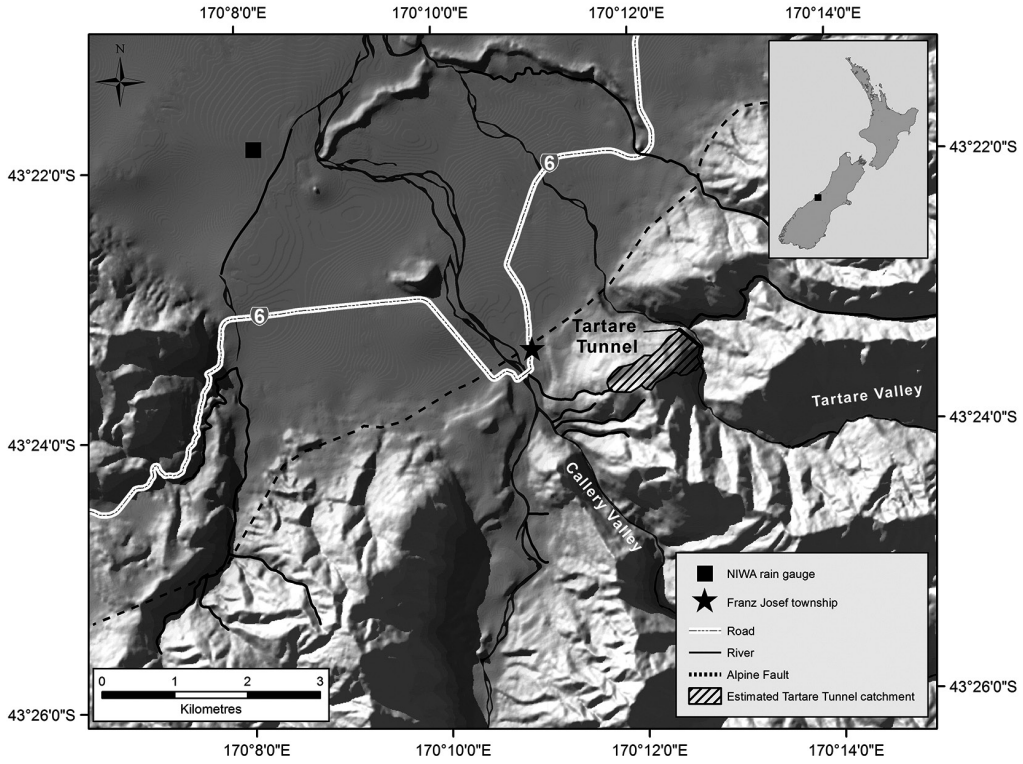

Figure 1 – Locations of the Tatare Tunnel on the western flanks of the Southern Alps and the NIWA rain gauge 5 km north-west of the Franz Josef township (black star) Westland, New Zealand. Approximate surface trace of the Alpine Fault is also shown (Cox and Barrell, 2007).

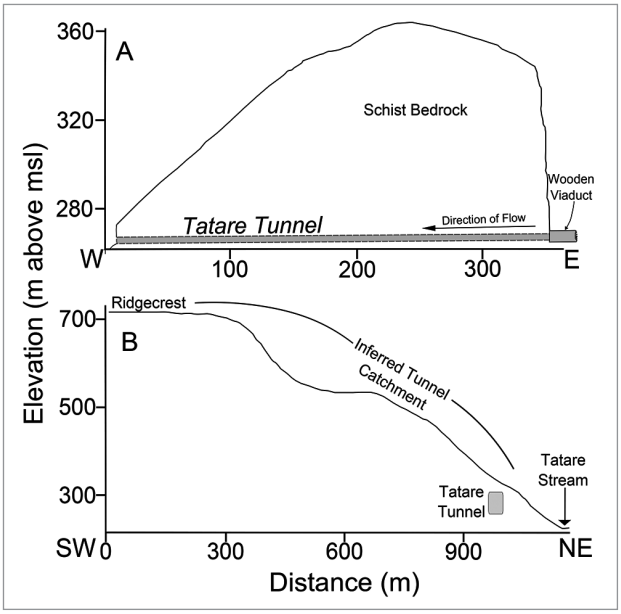

Figure 2 – (A) Longitudinal cross section of the Tatare Tunnel showing depth of overburden and position of outlet and, (B) valley-normal cross section of the inferred Tatare Tunnel catchment illustrating the position of the tunnel within the hillside. Topographic data derived from the NZSoS DEM (Columbus *et al.*, 2011).

Observations and measurements

Discharge measurements

Water depth and velocity were measured at 15-minute intervals with a flat-mounted, Unidata Starflow Ultrasonic Doppler Instrument (model 6526) sensor installed on the floor of the outflow half-pipe (Appendix A). The depth of water exiting the tunnel did not exceed the radius of the half pipe at any time during the study. The water depth and velocity measurements were converted to discharge estimates with an equation that assumes flow in a pipe that is less than half full (Appendix A). Tunnel discharge was monitored continuously between April 2012 and January 2013 to capture storm events typical of autumn and spring (March to May, and September to November, respectively) as well as of the cool, dry winter months (June to August) and the period of maximum rainfall during summer (December to January).

Rainfall totals, recorded at 15-minute intervals, were obtained from an automatic weather station (network no. F30313) 5 km north-west of Franz Josef township (NIWA, 2013) (Fig. 1). Because the rain gauge was not designed to directly record snowfall, precipitation records could not be separated into rainfall and snowmelt components. The precipitation data used in this study, therefore, reflects both rainfall and melted snow that accumulated in the gauge. Observations of fresh snow lying on the ground near the study site, however, provided evidence for snowfall settling at the altitude of the tunnel. Snow also fell at higher altitudes during the cool winter months.

A total of 3110 mm of precipitation was recorded by the rain gauge between April 2012 and January 2013 (NIWA, 2013). The spring and summer months showed larger totals and greater tunnel discharges than the drier autumn and winter months (Fig. 3, Table 1). The summer readings included a rainstorm on 1-3 January 2013, with an estimated return period of ten years (Tait *et al.*, 2012), that was experienced throughout the Westland region. The winter months

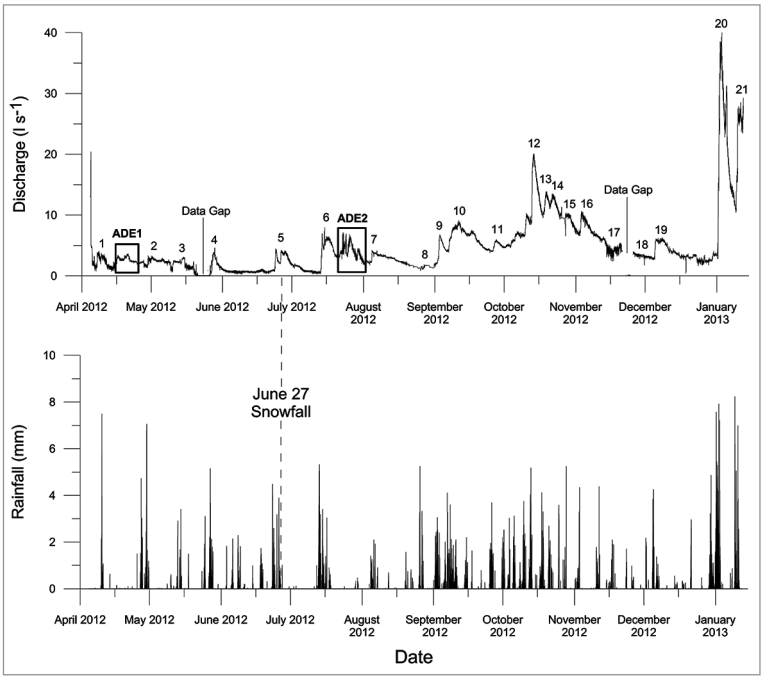

Figure 3 – Tatare Tunnel discharge hydrograph, with the discharge events and the two Anomalous Discharge Events identified. 15-minute rainfall records at the NIWA rain gauge for the period April 2012 to January 2013 are also shown. The snowfall of 27 June 2012 is annotated. The gauge at Franz Josef was not designed to accurately record snowfalls. Numbers refer to discharge events.

of 2012 were unusually dry throughout Westland, and soil moisture content was correspondingly low, yet Franz Josef township received its largest snowfall in 18 years on 27 June 2012 (Mills, 2012).

Table 1 – Characteristics of rainfall and tunnel discharge for all 21 discharge events. Negative values occurred when an increase in tunnel discharge precedes the onset of rainfall at Franz Josef. Modelled values (percent of rainfall infiltrated) assume a catchment area of 0.54 km^2 (Fig. 1).

Discharge Event	Total rainfall (mm)	Mean rainfall intensity (mm/hr)	Cumulative tunnel discharge (Q_c) (L)	Peak discharge (L/s)	T_1 (hr)	T_2 (hr)	Modelled percentage of rainfall infiltrated (%)
1	66.9	2.9	582	4.0	-35	-44	1.6
2	128.4	2.6	1050	3.3	22	11	1.5
3	75.2	2.1	231	3.0	7	6	0.6
4	215.2	0.5	2097	4.6	-1	-8	1.8
5	128.9	2.5	2097	4.5	14	17	4.0
6	299.9	3.8	2857	7.9	17	15	1.7
7	82.6	1.3	2699	4.2	0	-4	2.3
8	85.3	2.9	1025	1.8	8	10	0.3
9	198.3	4.0	1384	6.7	-28	12	1.3
10	185.6	1.7	7796	9.2	42	75	7.7
11	271.6	2.4	4903	7.3	22	36	3.3
12	268.9	3.9	7483	20.0	20	16	5.1
13	102.4	2.5	2810	13.8	25	38	5.0
14	81	2.8	3801	13.5	8	22	8.6
15	34.4	1.4	3809	10.3	20	10	20.3
16	103.2	1.7	6813	10.6	31	8	12.1
17	37.8	2.0	1137	5.4	4	79	5.5
18	53.7	2.0	2781	4.0	33	42	9.5
19	161.5	1.8	7989	6.3	-5	18	9.0
20	355.7	4.0	15485	40	22	15	7.9
21	145.4	4.4	6601	29.2	4	12	8.3
Mean	146.7	2.5	4068	10.0	11	18	5.6

Two assessment criteria must have been met to define a discharge event (DE): (a) a discernible rainfall pulse of over 10 mm within 24 hours (termed a rainstorm), and (b) an abrupt increase in tunnel discharge beyond baseflow values (Fig. 3). Time delays between the start of a rainfall pulse and the beginning of increased tunnel discharge resulted in overlap between some discharge events. Figure 4 shows graphically how individual discharge events were identified from the discharge record. Total rainfall (mm), the duration of rainfall (hours), the time interval between the onset of rainfall and the upward inflection of the discharge hydrograph (T_1), and the interval between peak rainfall and peak tunnel discharge (T_2) – both in hours – were noted for each discharge event (Table 1).

The assumption that tunnel discharge was driven solely by rainfall that fell during the corresponding event is unlikely to hold true for all discharge events. Changes in the dominance of celerity vs. velocity effects in the rock mass mean that the transmission time of a rainfall signal from the surface to the tunnel will vary between events. However, while antecedent rainfall is likely to drive some discharge in subsequent events, it is assumed to be a small driver compared to rainfall immediately prior to the discharge event.

Between April 2012 and January 2013, the temperature of water entering the Tatare Tunnel was 9.8 ± 0.5°C (Sims, 2013) and tunnel discharge ranged between 0.09 L/s and 40.01 L/s. While tunnel discharge responded to almost all the identified rainfall events, with the rising limbs of the associated hydrographs often nearly vertical, the magnitude and character of a response – given by the shape of a discharge hydrograph – were not uniform across the period (Fig. 3). The discharge record shows a general increase in the volume of water entering the tunnel between DE9 (September 2012) and DE21 (January 2013) (Fig. 3), the latter half of the measurement period.

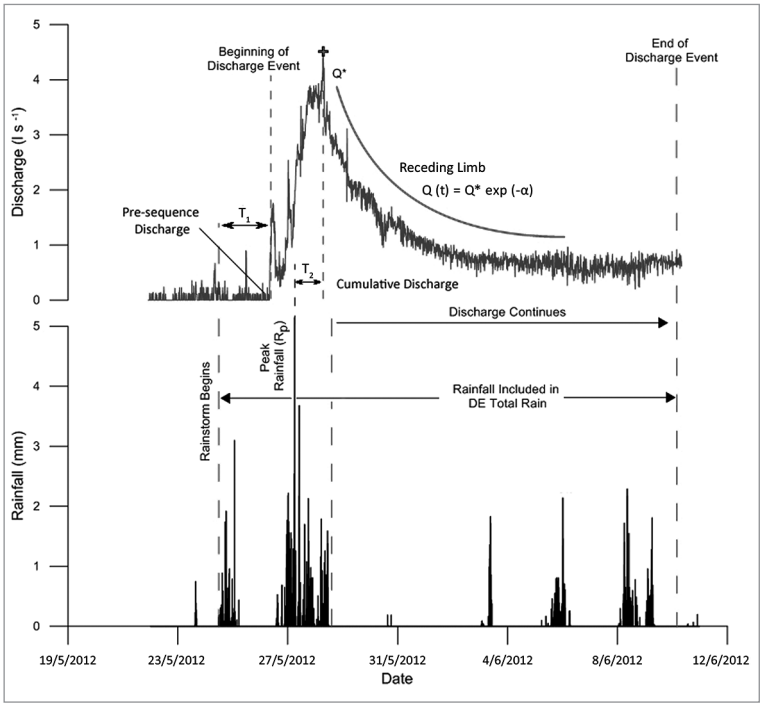

Figure 4 – A discharge event with the main components annotated. 'Pre-sequence' discharge is the absolute flow at the beginning of the event and was used when calculating cumulative tunnel discharge (the area under the discharge curve) for each of the 21 events identified. T_1 and T_2 refer to the time interval between the onset of rainfall and the onset of increased tunnel discharge, and the time interval between peak rainfall and peak tunnel discharge, respectively.

Tunnel inflows

Zones of groundwater seepage from the tunnel walls and roof showed as flow from open fractures and as slow dripping. Many such zones were observed to expel water only during rainfall events. While drip-zones were more common than larger open fractures, the latter had significantly greater inflow rates. A fracture on the true left wall, approximately 50 m from the tunnel's western entrance, showed significantly greater discharge than any of the other seepage areas with water flowing from them in August, September, October and January, regardless of precipitation totals at the time.

Anomalous discharge events

An exceptional event, labeled 'Anomalous Discharge Event 2' (ADE2) in Figure 3, was observed in July 2012, for which the rising limb was notably less steep compared to that of the other recognized events. A similar situation, albeit of shorter duration and lesser magnitude, was observed in early April 2012 (ADE1 in Figure 3). The two anomalous discharge events are shown in more detail in Figure 5. In both instances there was significant rainfall before and after increased tunnel discharge, even though little rain fell during the period of maximum discharge. Rapid fluctuations in discharge were noted for ADE2. Water depth and velocity data for this period show that these fluctuations resulted from rapid changes in the depth of water in the tunnel outflow pipe, preceding changes in water velocity. The cause of these rapid, short-lived fluctuations is not immediately obvious, and they were not observed at any other time during the study period. We rule out human interference given their longevity, and suggest localized channel blockage or damming was responsible.

Analysis

Discharge events

In general, the magnitude of peak discharges were markedly lower in period one (April to August 2012) than in period two (September 2012 to January 2013), even though the event precipitation totals were similar (Fig. 3). Either the amount of infiltration at the surface was less between April and August 2012, compared with that between September 2012 and January 2013, or surface infiltration remained relatively static and less of the infiltrated water directly induced a

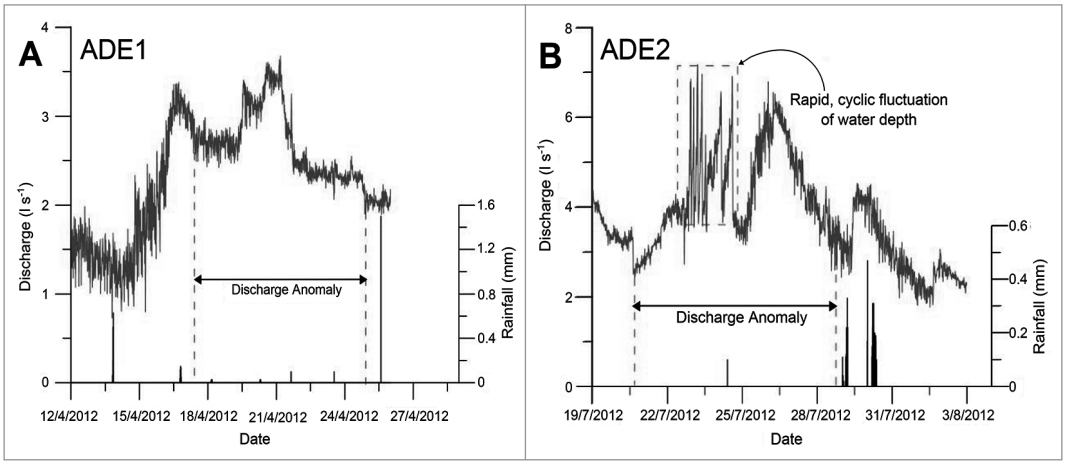

Figure 5 – (A) Anomalous Discharge Event 1 (ADE1) in April 2012 and, (B) Anomalous Discharge Event Two (ADE2) in June/July 2012, as identified in Figure 3. During these events, tunnel discharge increased in the apparent absence of rainfall.

change in tunnel discharge. Snow or ice at higher altitudes during the winter months of April to August 2012 may account for the reduced infiltration, although much of the likely tunnel catchment area lies below the elevation of the winter snowline (1570 m). Alternatively, some downward percolating water may have moved into storage within the rock mass following infiltration, thereby reducing the amount that would reach the tunnel during a discharge event.

Timing of Discharge Events

Time measurements for discharge events (Fig. 6) show a general shift in T_1 and T_2 values between the two periods, April to August 2012 (DEs 1-8) and September 2012 to January 2013 (DEs 9-21). These changes mirror the changes in peak tunnel discharge summarised in Figure 3. Precipitation events in the April to August 2012 period had much lower values of T_1 and T_2 than did those in the September 2012 to January 2013 period (Fig. 6). The dashed line in Figure 6 delineates the shift in T_1 and T_2 values between the two periods.

Rather than being a proxy for the transmission time of water from the surface to the tunnel, the highly variable T_1 and T_2 values – which include negative values – are a function of the mismatch between the timing of precipitation on the Westland coastal plain, where the rain gauge is located, and the onset of rainfall in the foothills of the Southern Alps approximately 7 km away. Although the change in T_1 and T_2 values between periods one and two coincides with the general increase in peak discharge magnitude described above, variations in the distribution of rainfall are likely the main determinant of the T_1 and T_2 values, not changes in the rate or proportion of precipitation infiltrating the rock mass. Values are in the order of hours to days and, because orographic rainfall likely begins earlier at higher elevations, they provide an upper limit to tunnel response time.

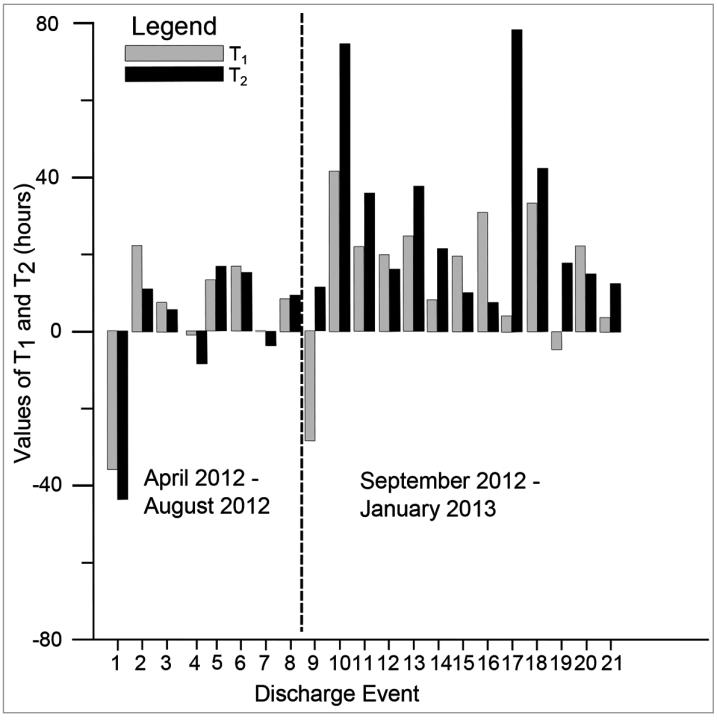

Figure 6 – Time intervals T_1 and T_2 for all 21 discharge events. DEs for April to August 2012 generally show markedly lower values (including several instances when discharge peaked before rainfall) than those in September 2012 to January 2013. The dashed line separates discharge events between the two periods.

Discharge model

Discharge events (Figs. 3 and 4) were used in a numerical model to compare volumes of tunnel discharge induced by different rainstorms. The cumulative discharge of the tunnel during a discharge event is assumed to have been induced by a particular rainfall event. It was assumed that differences in volumes of water that reached the tunnel walls during discharge events reflected differences in patterns of infiltration, the rate at which water moves through the rock, and degree of saturation of the rock mass surrounding the tunnel. Quantification of cumulative discharge allowed description of infiltration patterns and enabled comparison of discharge events. For calculation of cumulative tunnel discharge, represented by the area under the tunnel hydrograph in Figure 4, the following formula was used:

$$Q_c = \sum_{t=1}^{n} (Q_t \times 60 \times 15)$$

where Q_c is cumulative tunnel discharge in excess of 'pre-sequence discharge', measured in litres; $t = 1$ is the start of a discharge event; $t = n$ is the end of a discharge event; and Q_t is average tunnel discharge for each 15-minute measurement, measured in L/s. 'Pre-sequence discharge', defined as the discharge rate immediately preceding a sequence of discharge events, was held constant throughout the calculations (Fig. 4).

Figure 7 shows calculated cumulative discharge against rainfall total for each of the 21 discharge events. Cumulative discharge increased with total rainfall, but at a greater rate between September and January than between April and August. With the exception of DE5 – the precipitation total of which was presumably under-recorded due to the rain gauge's inability to accurately record snowfall separately from rainfall – values of cumulative tunnel discharge between April and August lie close to the linear trend line of form $Q_c = 10\,TR - 21$. Events between September and January generally have greater cumulative discharge values but show more scatter about the trend line $Q_c = 27\,TR + 1407$.

During the second period, much more water arrived at the tunnel per unit of rainfall than was the case for many of the precipitation events between April 2012 and August 2012. One explanation for this is that physical variations in surface conditions affected the source and efficiency of infiltration: for example, due to ice or snow cover or soil/rock saturation. Alternatively, subsurface variations in the source of discharged water, with some changes in the groundwater flow regime, were experienced. Clearly there was a change in discharge characteristics between the two periods, and this is mirrored in the discharge patterns depicted in Figure 3, as well as the T_1 and T_2 metrics shown in Figure 6.

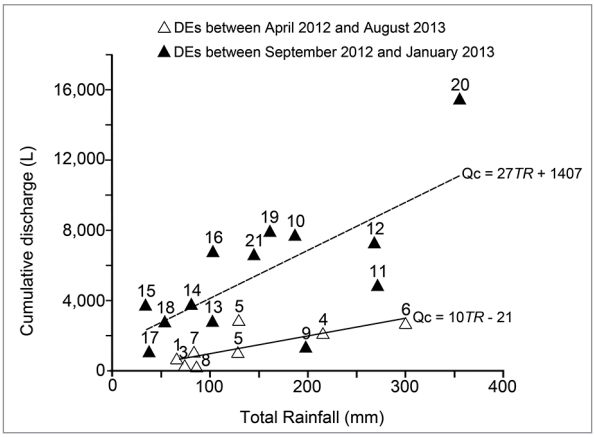

Figure 7 – Total rainfall vs. cumulative tunnel discharge for each of the 21 discharge events. Open triangles are discharge events between April and August 2012 and closed triangles are events between September 2012 and January 2013.

Calculated values of cumulative tunnel discharge were used in a simple numerical model to estimate the proportion of total precipitation that infiltrated the rock mass, and, presumably, recharged groundwater. Several assumptions were made before the model could be applied. First, 15-minute rainfall totals (mm) recorded at the rain gauge were assumed to apply across the tunnel catchment. Second, it was assumed cumulative discharge from the Tatare Tunnel was driven by infiltration during the concurrent rainstorm. Third, although the actual groundwater catchment area is unknown, it was assumed that it was directly related to surface topography and that catchment boundaries could be mapped from the shape of topographic features. We further assumed that catchment area did not change between storm events.

The equation used to calculate infiltration proportions was:

$$I_P = \frac{Q_E}{V_R}$$

where *IP* is the proportion of precipitation in a discharge event that infiltrates the rock mass to drive discharge in the Tatare Tunnel; *QE* is cumulative discharge during the discharge event, in litres; and *VR* is the total volume of rainfall for the designated catchment area, in litres. *QE* was calculated with the following equation:

$$QE = \sum_{t=1}^{n} [Q_t - Q_{PS}]$$

where $t = 1$ is the start of the discharge event; $t = n$ is the end of the discharge event; Qt is tunnel discharge at time t; and QPS is the baseflow discharge ('Pre-sequence Discharge' in Figure 4) during the discharge event at time t. Q_E is expressed in litres and Q_t and Q_{PS} are expressed as L/s. *VR* was calculated from the following equation:

$$V_R = [A \times R_d] \times 1000$$

where A is catchment area, in m^2; R_d is rainfall in metres; and is in litres.

Topographic divides are often assumed to coincide with groundwater flow divides, so the Digital Elevation Model (DEM) derived by Columbus *et al.* (2011) was used to map the margins of the catchment area. The lower boundary of the catchment area was defined by the trace of the tunnel, with its margins set by small ridges perpendicular to the Tatare Valley. The upstream boundary was the ridge crest above the tunnel that separated the Tatare and Callery Valleys (Fig. 1). Catchment area was estimated to be 0.54 km^2.

The proportion of rainfall that infiltrated the rock mass was then calculated for each discharge event. The proportion of rainfall infiltrating during each discharge event varied between 0.3% and 20% (Table 1). Discharge events between September 2012 and January 2013 generally had greater (> 5%) percentages of infiltrated water than those between April and August 2012.

Discussion

Discharge response to rainfall

The observed rapid response of tunnel discharge to a precipitation event (Fig. 3) is consistent with groundwater flow through a highly fractured, 'decompressed' zone in the rock mass traversed by the Tatare Tunnel (Marechal and Etcheverry, 2003). The regolith overlying the tunnel is thin and/or likely to be regularly near-saturated, meaning that rock below the soil-rock interface is likely to control the rate and volume of discharge in the tunnel. In Otago, the structure of schist is known to exert a strong influence on rates and patterns of infiltration within ~5 m of the surface (Gillon *et al.*, 1992; Macfarlane *et al.*, 1992), as well as infiltration-related cooling of water in nearby hot springs in the Southern Alps (Cox *et al.*, 2015).

Orographic rainfall and snowmelt

The two anomalous discharge events identified in April and July 2012 (Fig. 5) suggest

that the rainfall records used for the study may not always be indicative of rainfall in the Tatare Tunnel catchment, and/or rainfall may not be the only source of water for discharge. Isolated rainfall recharge and snowmelt infiltration are discussed further in this section.

The steep rainfall gradients of the Southern Alps mean that while orographic rain may fall high in the mountains, the area surrounding the gauge near Franz Josef township could remain relatively dry (Griffiths and McSaveney, 1983). The rainfall gradient steepens rapidly at altitudes above 500 m (Anderson *et al.*, 2006), and the rain gauge is at 90 m above msl. Spatially-confined rainfall events could have occurred in the tunnel catchment, yet might not have been recorded by the rain gauge. Differences in the timing and volume of rainfall received at the rain gauge compared with at the Tatare Tunnel are possible at any time of the year, but the difference is expected to be greatest during larger storm events from the west; a number of such events occurred in quick succession during the spring and summer months of 2012/2013 (Fig. 3). Values of T_1 and T_2 in the five-month period between April and August 2012 may be more representative of the true tunnel response time because mismatch between rainfall at the gauge and that above Tatare Tunnel is expected to be less during the winter months.

The most striking difference between the discharge hydrograph of a typical recharge event and that for an anomalous discharge event lasting nine days or more was the hydrograph shape. During an anomalous discharge event, the rising and falling limbs had gentle slopes and the ADE2 peak discharge was relatively subdued compared to flow rates immediately before and after. Kresic and Bonacci (2010) showed how water from an isolated recharge event can travel through a rock mass and be expressed in a spring discharge hydrograph as suppression of the peak and an increased spread of discharge over time (Fig. 8). Records of anomalous discharge events in the Tatare Tunnel show strong similarities to such a signal.

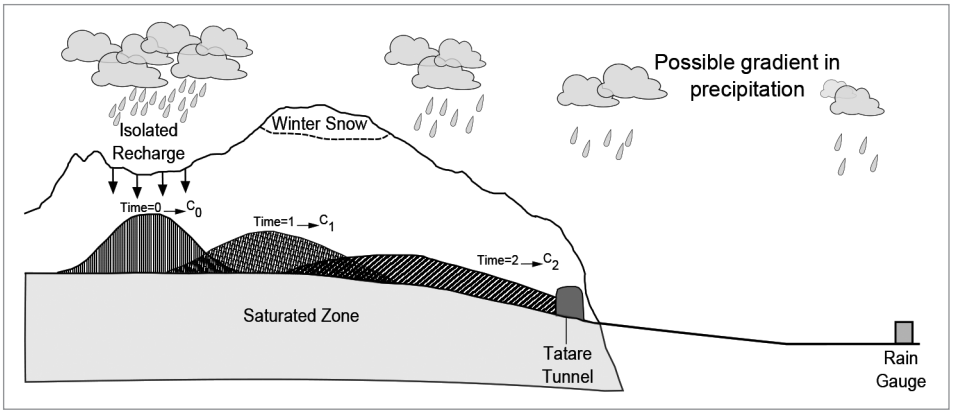

Figure 8 – Possible explanations for the anomalous discharge events observed in the Tatare Tunnel discharge record: rainfall gradient between the rain gauge and the tunnel catchment and a highly localised recharge event leading to the formation and subsequent movement of a groundwater 'wave', where t is time and C is wave velocity. Wave velocity includes both celerity effects and mean velocity of water percolating through the bedrock. Water that recharges the Tatare Tunnel during such events may be 'old' water discharged under the pressure of the recharge wave. Adapted from Kresic (2010).

On June 27 2012, Franz Josef experienced its heaviest snowfall in 18 years (Mills, 2012), and the total of 128 mm recorded in the rain gauge during DE5 incorporated water from both rainfall and snowmelt. This storm brought 18 cm of snow to sea level in the Franz Josef region, and informal observations showed that much of that snow remained on the forest floor above Tatare Tunnel for at least two weeks (D. Waters, DoC, pers. comm. 30/08/2012). DE5 also had the highest proportion of precipitation infiltrated of all discharge events between April and August 2012 (Table 1).

Anomalous Discharge Event 2 (ADE2) in July-August 2012 followed this rain-on-snow DE6 event. Snowmelt is sensitive to an increase in atmospheric temperature and an increase in latent heat flux associated with the melting of surface snow during a rainfall event (Anderson and Mackintosh, 2012; Ishikawa *et al.*, 1992; Marcus *et al.*, 1985). When rain falls on a snowpack, flows of liquid water, infiltration rates and groundwater flows commonly peak after a delay of several days. The snowmelt hydrographs analysed by Gardner *et al.* (2010) are similar in slope and duration to those for the anomalous discharge events observed at Tatare Tunnel. Concurrently with ADE2, and for the period when snow was observed on the forest floor, a rapid rise in air temperature was reported at 500 m in the Callery Valley adjacent to the Tatare catchment (T. Kerr, NIWA, pers. comm. 31/10/2012). This suggests that snowmelt probably occurred during ADE2.

The impact of irregularly distributed rainfall and/or snowmelt may explain some of the complexity in the discharge hydrographs for Tatare Tunnel. Orographic rainfall can occur at any time whereas snowmelt infiltration is more likely during the winter and spring months. If this is correct, then it is likely that snowmelt was an important source of shallow groundwater in the hillside above the Tatare Tunnel during discharge events between June and November 2012.

Water table position

The main finding of the observations and calculations involved in this research was that discharge events between September 2012 and January 2013 were associated with larger values of cumulative tunnel discharge per unit of rainfall than for storms between April and August 2012 (Fig. 7). This was also evident in the infiltration modelling, which showed a relatively large proportion of rainfall infiltrated for most storms between September 2012 and January 2013 (Table 1). The modelling indicates that, compared with discharge events between April and August 2012, more water entered the tunnel in a shorter time during precipitation events from September 2012 to January 2013. Two mechanisms may account for this. First, physical differences at the surface of the catchment could have led to differences in infiltration rates between the two periods. Secondly, not all of the water that reached the tunnel during a discharge event might have been driven directly by water infiltrating the rock mass above the tunnel during that event.

Snow-armouring, or ice lying close to the surface, can impede the infiltration of rain water (de Vries and Simmers, 2002). However, there is no record of sub-surface ice across the Tatare Tunnel catchment, and there is no evidence of a sudden decline in snow cover between the April to August and the September to January periods.

Saturation of the rock mass that surrounds the tunnel may explain the increase in the volume of tunnel discharge initiated per unit of rainfall between September 2012 and January 2013. As the water table in the hillside rises, differences in pressure head between the tunnel (atmospheric) and the surrounding rock mass (hydrostatic) can be expected to drive groundwater towards the tunnel (Masset and Loew, 2010; Rybach, 1995). The observed flow of water from fractures in the bed of the tunnel in October 2012 and January 2013 suggests variations in

the source of discharge. Seepage up through the tunnel floor indicates that the water table was then above the elevation of the tunnel floor and that fluid was being driven towards the tunnel by differences in pressure head between the surrounding rock mass and the tunnel. If the water table lies close to the tunnel, then it will control the timing and volume of discharge.

Discharge patterns observed between September 2012 and January 2013 suggest that the water table was elevated at that time. We suggest that during this period, the source of tunnel discharge was not only downward percolating fluid but also the lateral movement of water in the hillside. Therefore, rainfall can be both a source of tunnel discharge and a hydraulic driver for expelling fluid stored in the rock mass into the tunnel (Walton-Day and Poeter, 2009). This suggests that the modelled proportions of rainfall infiltration during this period are overestimates compared with what might be derived elsewhere in the western Southern Alps.

Seasonality

The anomalous discharge events shown in Figure 5 suggest that rainfall was not the sole source of water for tunnel discharge. Isotopic analyses suggested that groundwater was derived from a mixture of rainfall and snowmelt (Appendix B). Although no water samples were collected during ADE1 or ADE2, the results for ADE2 are consistent with snowmelt feeding the Tatare Tunnel. If this interpretation is correct, then water flowing through the tunnel between September 2012 and January 2013 must have begun to infiltrate the rock mass during the preceding winter.

Anomalous Discharge Event 2 (ADE2) is interpreted as the consequence of infiltrating snowmelt associated with variations in rainfall and temperature at the surface. Snowmelt infiltration is likely a significant contribution to rock-mass saturation and a cause of elevation of the water table surrounding the tunnel. In this manner, snowmelt forces water stored in the rock mass to become a significant driver of tunnel discharge. Figure 9 illustrates movement of infiltrating water into storage within the rock mass as well as the passage of groundwater from surface to tunnel. Seasonal variations in snowfall, and hence snowmelt infiltration, may give rise to seasonal-scale changes in water table elevation. If this is the case then snowmelt infiltration may directly influence tunnel discharge at the timescale of individual events

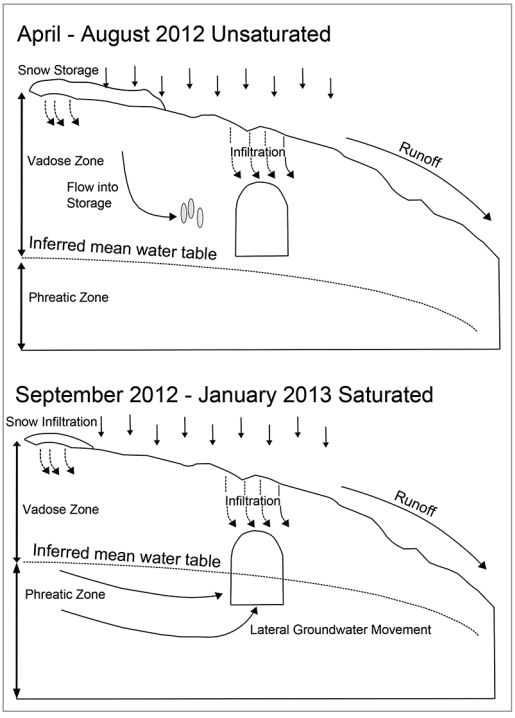

Figure 9 – Schematic summarising the change in patterns of groundwater flow between the periods April to August 2012 and September 2012 to January 2013. Water was forced into storage during the drier winter months and an increase in the elevation of the water table in spring and summer could result in greater tunnel discharge during a rainfall event when water flowing laterally through the saturated zone may be intercepted by the Tatare Tunnel.

(days) and indirectly via seasonal shifts in the position of the water table (months).

Future research

The T_1 and T_2 metrics provide an upper bound to groundwater response time, and the discharge hydrographs patterns shed light on the magnitude of this response. This recharge signal is influenced by both celerity and velocity of the groundwater system (McDonnell and Beven, 2014). These factors are in turn influenced by the hydraulic conductivity, storage properties and degree of saturation of the rock mass (Kirchner, 2003). To move beyond the first-order insights presented here is not straightforward. It would need a comprehensive study employing both discharge measurements and hydrological tracers that would not be simple to deploy in this steep, rugged, mountainous, forested area of Westland National Park.

Conclusions

Discharge of groundwater in Tatare Tunnel, through the schist hanging wall of the Alpine Fault, was measured between April 2012 and January 2013. Measurements of discharge were compared with rainfall recorded at the NIWA rain gauge 7 km north-east of the tunnel. Our key conclusions are:

1. Tunnel discharge typically responded rapidly to precipitation events, and showed a clear difference in timing and magnitude characteristics between the periods April 2012 to August 2012 and September 2012 to January 2013.
2. Anomalous discharge events, recorded on two occasions, are interpreted as the consequence of infiltration of snowmelt or highly localised orographic rainfall.
3. Discharge events between September 2012 and January 2013 showed markedly higher values of cumulative and peak discharge per unit rainfall than events between April and August 2012. This shift in discharge characteristics was likely driven by the rise and fall of the water table in the rock mass surrounding the tunnel.
4. The tunnel groundwater catchment area was assumed to be 0.54 km^2, on the basis of surficial topographic boundaries. Calculations indicate that between 0.3% and 20% of precipitation infiltrated the schist rock mass during the study period.

Future research is needed for better understanding the link between snowfall, snowmelt and patterns of groundwater flow. Stable isotope analyses, or the use of another appropriate tracer, would better establish this link.

Acknowledgements

The authors thank Damon Teagle, Catriona Menzies, Dave Craw and Michael Manga for their help in refining the project and identifying its target audience. Additionally we wish to thank the two anonymous reviewers for providing constructive feedback on this manuscript and Richard Hawke – the editor of Journal of Hydrology (NZ) – for facilitating publication. This research was made possible by a grant from the NZHS project fund. The authors also thank: Dave Waters (Department of Conservation, Franz Josef) for assisting with field logistics; NIWA Cliflo database and Tim Kerr (NIWA, Christchurch) for providing rainfall data and encouragement; Rupert Sutherland (GNS Science, Avalon) for advice and field support; Julie Clark, Nigel McDonald and Dave Howarth (University of Otago, Geography Department, Dunedin) for assistance with laboratory work and field equipment; Robert Van Hale (University of Otago, Chemistry Department, Dunedin) for assistance with stable isotope analyses; staff at Dunedin office of GNS Science for constructive feedback throughout the research; and Oliver O'Sullivan, Tom Baker and Katherine Lyttle for assistance in the field.

References

Anderson, B.; Lawson, W.; Owens, I.; Goodsell, B. 2006: Past and future mass balance of 'Ka Roimata o Hine Hukatere' Franz Josef Glacier, New Zealand. *Journal of Glaciology 52(179):* 597-607

Anderson, B.; Mackintosh, A. 2012: Controls on mass balance sensitivity of maritime glaciers in the Southern Alps, New Zealand: The role of debris cover. *Journal of Geophysical Research 117*: 1-15

Bickle, M. J.; McKenzie, D. 1987: The Transport of Heat and Matter by Fluids During Metamorphism. *Contributions to Mineralogy and Petrology 95*: 384-392

Columbus, J.; Sirguey, P.; Tenzer, R. 2011: A free, fully assessed 15-m DEM for New Zealand. *Surveying Quarterly 66*: 16-19

Cox, S.C.; Barrell, D.J.A. (compilers) 2007: Geology of the Aoraki Area, New Zealand. Institute of Geological & Nuclear Sciences 1:250,000 geological map 15. 1 sheet + 71p. Lower Hutt, New Zealand, GNS Science.

Cox, S.C.; Menzies, C. D.; Sutherland, R.; Denys, P. H.; Chamberlain, C. A.; Teagle, D. A. H. 2015: Changes in hot spring temperature and hydrogeology of the hanging wall of the Alpine Fault, New Zealand, induced by distal South Island earthquakes. *Geofluids 15(1-2)*: 216-239

Cox, S.C.; Stirling, M. W.; Herman, F.; Gertsenberger, M.; Ristau, J. 2012: Potentially active faults in the rapidly eroding landscape adjacent to the Alpine Fault, central Southern Alps, New Zealand. *Tectonics 31*: 1-21

Cox, S.C.; Sutherland, R. 2007: Regional Geological Framework of South Island, New Zealand, and its Significance for Understanding the Active Plate Boundary. *In*: Okaya, D; Stern, T.; Davey, F. (*eds*.) *A Continental Plate Boundary: Tectonics at South Island, New Zealand*. American Geophysical Union, Washington D.C.

De Vita, P.; Reichenbach, P.; Bathurst, J.C.; Borga, M.; Crosta, G.; Crozier, M.; Glade, T.; Guzzetti, F.; Hansen, A.; Wasowski, J. 1998: Rainfall-triggered landslides: a reference list. *Environmental Geology 35*: 219–233

de Vries, J. J.; Simmers, I. 2002: Groundwater recharge: an overview of processes and challenges. *Hydrogeology Journal 10*: 5-17

Gardner, W.P.; Susong, D. D.; Solomon, D. K.; Heasler, H. 2010: Snowmelt hydrograph interpretation: Revealing watershed scale hydrologic characteristics of the Yellowstone volcanic plateau. *Journal of Hydrology 383*: 209-222

Gillon, M.D.; Riley, P. B.; Haliday, G. S. 1992: Movement history and infiltration, Cairnmuir Landslide, NZ. *Proceedings of the Sixth International Symposium on Landslides*: 103-110

Glade, T. 1998: Establishing the frequency and magnitude of landslide-triggering rainstorm events in New Zealand. *Environmental Geology 35*: 160–174

Griffiths, G.A.; McSaveney, M. J. 1983: Distribution of mean annual precipitation across some steepland regions of New Zealand. *New Zealand Journal of Science 26(2)*: 197-209

Hicks, D.M.; Shankar, U.; McKerchar, A.; Basher, L.; Lynn, I.; Page, M.; Jessen, M.: Suspended Sediment Yields from New Zealand Rivers. *Journal of Hydrology (New Zealand)*, *50 (1)*: 81-142

Ibbitt, R.P.; Henderson, R.D.; Copeland, J.; Wratt, D.S. 2001: Simulating mountain runoff with meso-scale weather model rainfall estimates: a New Zealand experience. *Journal of Hydrology 239*: 19-32

Ishikawa, N.: Sturman, A.P.: Owens, I.F. 1992: Heat balance characteristics during fine periods on the lower parts of Franz Josef Glacier, New Zealand. *International Journal of Climatology 12*: 397-410

Kirchner, J.W. 2003: A double paradox in catchment hydrology and geochemistry. *Hydrological Processes 17*: 871-874

Koons, P.O.; Craw, D. 1991: Evolution of fluid driving forces and composition within collisional orogens. *Geophysical Research Letters 18(5)*: 935-938

Koons, P. O.; Craw, D.; Cox, S. C.; Upton, P.; Templeton, A. S.; Chamberlain, C. P. 1998: Fluid flow during active oblique convergence: A Southern Alps model from mechanical and geochemical observations. *Geology 26(2)*: 159-162.

Koons, P.O.; Norris, R. J.; Craw, D.; Cooper, A. F. 2003: Influence of exhumation on the structural evolution of transpressional plate boundaries: An example from the Southern Alps, New Zealand. *Geology 31(1)*: 3-6

Kresic, N.; Bonacci, O. 2010: Spring discharge hydrograph. In: Kresic, N; Stevanovic, Z. (*eds.*) *Groundwater Hydrology of Springs: Engineering, Theory, Management and Sustainability*. Elsevier, Burlington, MA

Macfarlane, D.F.; Pattle, A.D.; Salt, G. 1992: Nature and identification of the Cromwell Gorge landslides groundwater systems. *Proceedings of the Sixth International Symposium on Landslides 1*: 509-518

Marcus, M.G.; Moore, R.D.; Owens, I.F. 1985: Short term estimates of surface energy transfers and ablation on the lower Franz Josef Glacier, South Westland, New Zealand. *New Zealand Journal of Geology and Geophysics 28*: 559-567

Marechal, J.C.; Etcheverry, D. 2003: The use of ^{3}H and ^{18}O tracers to characterize water inflows in Alpine Tunnels. *Applied Geochemistry 18*: 339-351

Masset, O.; Loew, S. 2010: Hydraulic conductivity distribution in crystalline rocks, derived from inflows to tunnels and galleries in the Central Alps, Switzerland. *Hydrogeology Journal 18*: 863-891

McDonnell, J.J.; Beven, K. 2014: Debates- The future of hydrological sciences: A (common) path forward? A call to action aimed at understanding velocities, celerities and residence time distributions of the headwater hydrograph. *Water Resources Research 50*: 5342-5350

Menzies, C.D. 2012. Fluid Flow Associated with the Alpine Fault, South Island, New Zealand. PhD Thesis, University of Southampton

Menzies, C. D.; Teagle, D. A. H.; Craw, D.; Cox, S. C.; Boyce, A. J.; Barrie, C. D.; Roberts, S. 2014: Incursion of meteoric waters into the ductile regime in an active orogen. *Earth and Planetary Science Letters 399*: 1-13

Mills, L. 2012. Fifty-year snowfall on 'temperate' Coast. Greymouth Star, 27/06/2012

NIWA. 2013: CliFlo: NIWA's National Climate Database on the Web [Online]. Available: http://cliflo.niwa.co.nz/ 2015]

NIWA. 2014: New Zealand Climate Extremes [Online Resource]. Available: https://www.niwa.co.nz/education-and-training/schools/resources/climate/extreme

Purdie, H.; Bertler, N.; Mackintosh, A.; Baker, J.; Rhodes, R. 2010: Isotopic and elemental changes in winter snow accumulation on glaciers in the Southern Alps of New Zealand. *Climate 23*: 4737-4749

Rasmussen, T.C.; Baldwin, R.H.; Dowd, J.F.; Williams, A.G. 2000: Tracer vs. Pressure Wave Velocities through Unsaturated Saprolit. *Soil Science Society of America Journal 64*: 75-85

Rybach, L. 1995: Thermal waters in Deep Alpine Tunnels. *Geothermics 24(5/6)*: 631-637

Sharp, Z. 2007: *Stable Isotope Geochemistry.* Pearson Prentice Hall, New York

Sims, A. 2013: Shallow Fluid Movement in the Hanging Wall of the Alpine Fault. MSc Thesis, University of Otago

Stewart, M.K.; Cox, M.A.; James, M.R.; Lyon, G.L. 1983: *Deuterium in New Zealand Rivers and Streams*. Institute of Geological and Nuclear Sciences – DSIR, Wellington, New Zealand

Sutherland, R.; Toy, V. G.; Townend, J.; Cox, S. C.; Eccles, J. D.; Faulkner, D. R.; Prior, D. J.; Norris, R. J.; Mariani, E.; Boulton, C.; Carpenter, B. M.; Menzies, C. D.; Little, T. A.; Hasting, M.; De Pascale, G. P.; Langridge, R. M.; Scott, H. R.; Lindroos, Z. R.; Fleming, B.; Kopf, A. J. 2012: Drilling reveals fluid control on architecture and rupture of the Alpine Fault, New Zealand. *Geology 40*: 1143-1146

Tait, A.; Turner, R.; Chappell, P. 2012: National Climate Summary 2012. National Institute of Water and Atmospheric Research. Downloaded 15/01/ 2013 https://www.niwa.co.nz/climate/summaries/annual/annual-climate-summary-2012

Upton, P.; Sutherland, R. 2014: High permeability and low temperature correlates with proximity to brittle failure within mountains at an active tectonic boundary, Manapouri Tunnel, Fiordland, New Zealand. *Earth and Planetary Science Letters 389*: 176-187

Walton-Day, K.; Poeter, E. 2009: Investigating hydraulic connections and the origin of water in a mine tunnel using stable isotopes and hydrographs. *Applied Geochemistry 24*: 2266-2282

Wintsch, R. P.; Christoffersen, R.; Kronenberg, A. K. 1995: Fluid-rock reaction weakening of fault zones. *Journal of Geophysical Research: Solid Earth 100*: 13021-13032

Yardley, B. W. 2009: The role of water in the evolution of the continental crust. *Journal of the Geological Society 166*: 585-600

Appendix A: Discharge calculations

Tatare Tunnel discharge calculations

All water in Tatare Tunnel flows out a convenient old iron halfpipe left behind from a hydroelectric power scheme (Figure A1). The continuity equation was used to transform measurements of water velocity and depth at the Tatare Tunnel outlet, averaged at 15-minute intervals, to estimates of tunnel discharge. Mean velocity ($\bar{V}$) is measured directly by the Starflow instrument and the cross sectional area of flow in the half-pipe (A), is calculated from the equation:

$$A = \frac{r^2\left(\theta - sin\theta\right)}{2}$$

Where A is the cross sectional area of flow in m^2, r is the radius of the pipe in metres, and is calculated from water depth h, in metres, via the equation:

$$\theta = \cos^{-1}\left(\frac{r-h}{r}\right)$$

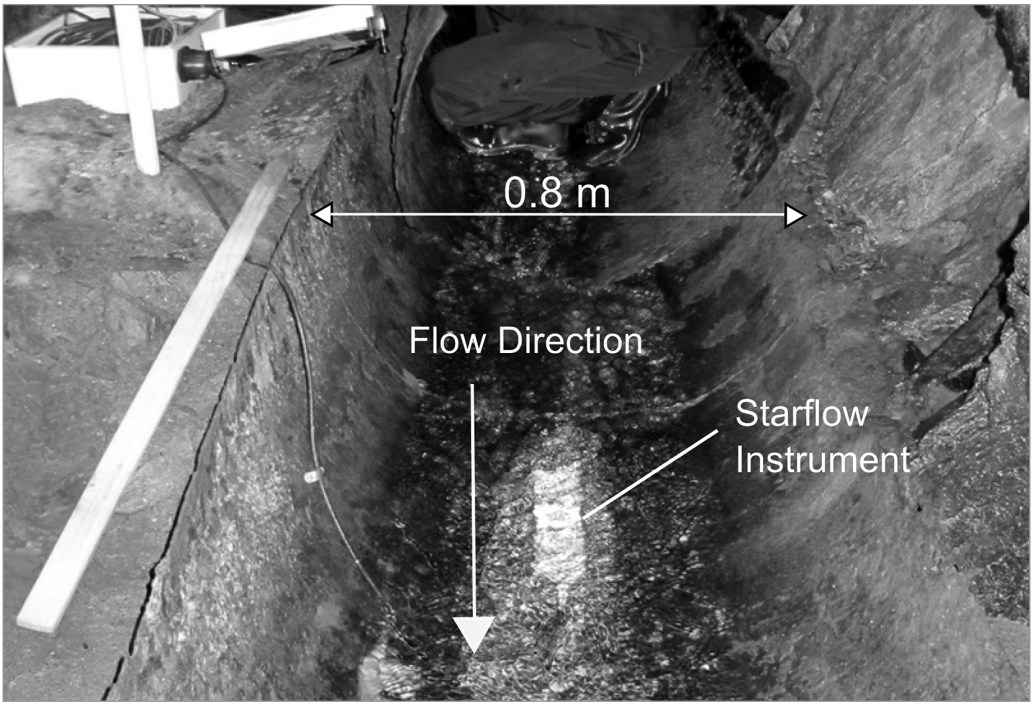

Figure A1 – Iron halfpipe in the bed of the Tatare Tunnel near its western portal. All water that enters the tunnel exits via this outlet and flows to the Tatare Stream below. Starflow Ultrasonic Doppler current Meter is attached to the tunnel bed. View is looking upstream.

Appendix B: Isotope analysis

In order to examine whether infiltration during winter-spring was derived from snow, rainwater, or a mixture of the two, 11 samples were collected from Tatare Tunnel for isotopic analysis during August 2012. A further two samples were taken in October 2012 and five in November 2012. Samples of water were collected from (a) current precipitation, (b) the Tatare Tunnel, and (c) nearby Tatare Stream. All water samples were stored in clean 30 ml polyethylene vials that had been filled to the top to exclude air, then sealed to avoid exchange between the sample and the atmosphere. Values of the ratio of $^{18}O/^{16}O$ and $^{2}H/^{1}H$ were determined using a *Picarro 2120* wavelength-scanned, cavity ring-down spectrometer in the Department of Chemistry, University of Otago. For each sample, eight aliquots were analysed and the raw results were numerically filtered by removing values beyond one standard deviation from the average. The revised average was corrected to the international Vienna Standard Mean Ocean Water (VSMOW) isotope scale by reference to the three-point calibration provided by three laboratory standards measured before and after every batch of 80 samples. The results are presented as values of $\delta^{18}O$ and δD relative to VSMOW. Details of analytic methods and standards adopted by the University of Otago Chemistry Department Laboratory are in Sims (2013).

Results from stable isotope analyses are plotted on Figure B1. The plot also includes a rainwater sample (Cox *et al.*, 2015) from Copland Valley, 30 km to the southwest, on 31 December 2009 to highlight the natural variability of $\delta^{18}O$ and δD in New Zealand rainwater. Rainwater values shift along the New Zealand Meteoric Water Line (NZMWL) according to the altitude and temperature at which water fractionates during nucleation (Sharp, 2007; Stewart *et al.*, 1983). A pronounced shift to lower values occurs when precipitation falls as snow or hail. Purdie *et al.* (2010) sampled the composition of snowfall on Franz Josef Glacier at 2300 metres above msl for 24 days in 2010. The mid-point of that sample distribution, and the bars indicating the range of sample values, are shown in Figure B1.

All water samples taken from Tatare Tunnel and Tatare Stream lie along the NZMWL mid-way between the rain and snow end-members. There is no evident shift in $\delta^{18}O$ values from this line, such as would occur if

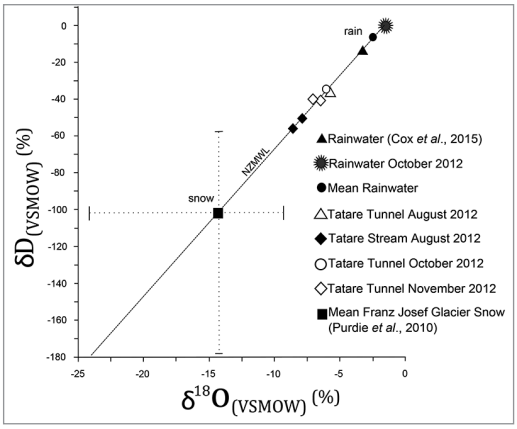

Figure B1 – δD vs. $\delta^{18}O$ values for rainfall and tunnel water samples taken throughout the measurement period. Franz Josef glacier snow and rainwater samples collected in the nearby Copland Valley (Cox *et al.* 2015) show the variability in δD and $\delta^{18}O$ values for New Zealand rainwater. All samples lie along the New Zealand Meteoric Water Line, indicating that infiltrating water has not undergone exchange with the rock mass surrounding the tunnel. Values are reported relative to Vienna Standard Mean Ocean Water (VSMOW). The simple mixing model used to infer the relative proportion of rain and snowmelt is also annotated.

there were exchange between the fluid and the schist rock mass (Menzies *et al.*, 2014). Although overlap between groundwater samples taken in August and October 2012 lies beyond the analytical uncertainties (approximately ±0.4 ‰ per mil $\delta^{18}O$ and ± 2‰ per mil δD), groundwater samples collected in November 2012 were consistently more depleted in lighter isotopes than their August and October counterparts. Displacement of individual sample values along the NZMWL toward the depleted end-member requires either a decrease in atmospheric temperature at which precipitation nucleates, or an increase in the relative amount of snowmelt in the groundwater. Shifts in the δD values of Tatare Tunnel water between August and November 2012 are within the expected seasonal variation of streams with a significant snowmelt input (Stewart *et al.*, 1983).

Manuscript received 4 February 2015 2014; accepted for publication 20 June 2015